

# Migration of $^{45}\text{Ca}$ and $^{90}\text{Sr}$ in a clayey and calcareous sand: Calculation of distribution coefficients by ion exchange theory and validation by column experiments.

France Lefèvre<sup>a</sup>, Michel Sardin<sup>b,\*</sup>, Pierre Vitorge<sup>a</sup>

<sup>a</sup> CEA Section de GéoChimie, B.P. 6, F-92265 Fontenay-aux-Roses Cedex, France

<sup>b</sup> CNRS LSGC, 1 rue Grandville, B.P. 451, F-54001 Nancy Cedex, France

Received 17 December 1993; accepted 15 December 1994 after revision

---

## Abstract

The transient transport of trace radiocalcium and radiostrontium in a clayey and calcareous sandy soil is mainly governed by: (1) cation exchange with the major cations on clay minerals; (2) calcocarbonic equilibria which control the concentration of calcium in the leaching solution; and (3) the initial composition of the leaching solution. If there are no changes in the concentration of the major cations and pH and ionic composition are stable, it is possible to calculate a distribution coefficient ( $K_d$ ) as a function of the major cations. In a constant physicochemical environment, this coefficient can be introduced in a linear transport model. Chromatographic experiments have been performed in which pulse injections of radiostrontium or radiocalcium are made into sand columns fed with various leaching solutions. The results are compared: (1) with the simulations based on a complete speciation model; and (2) with predictions from a linear model including the previously calculated  $K_d$ . The shape and the location of radionuclide peaks are well simulated for a large range of ionic composition ( $10^{-3}$ – $10^{-1}$  M for a mixture of  $\text{CaCl}_2$  and  $\text{NaCl}$ ).

The distribution of clay minerals in the porous medium is of great importance. The local equilibrium assumption only holds when clay minerals particles are uniformly distributed on the sand grains. Kinetic effects occur when clays are in the form of aggregates. These effects are evaluated by means of a first-order transfer model and by comparison with tracer tests at different flow rates.

---

\* Corresponding author.

## 1. Introduction

Predictive calculation of radioelement migration is needed to assess the security of radioactive waste disposals. The transport of radioactive solutes in groundwaters is usually governed by two coupled processes: the water flow and the physicochemical interactions between solutes and porous media. Local equilibrium is usually assumed when modeling radioelement migration, but kinetic processes can occur which change the shapes of breakthrough curves (Schweich and Sardin, 1981). The transport of linearly interacting solutes can be easily modeled by taking into account mass transfer limitations due to diffusion processes around (external diffusion) or within (internal diffusion) the aggregates of the porous medium (Sardin et al., 1991). Often the mass transfer limitations can be lumped in a overall first-order approximation involving a single characteristic time for mass transfer.

In radionuclide transport, the sorption of cationic species at low concentration can be measured in terms of a partition coefficient  $K_d$ , which is often assumed to be constant in transport models. Unfortunately,  $K_d$ -values depend on the chemical conditions which usually vary during transport. These variations are essentially due to the competition between the species under study and the major cations in solution at the adsorption sites. This competition can be taken into account by ion exchange theory. Strontium and calcium exchange on clay minerals have been successfully modeled by a mass action law (Heald, 1960; Gheyi and van Bladel, 1975). In a recent paper, Lefèvre et al. (1993) checked such predictions for strontium transport eluted by calcium solution in a chromatographic column filled with a stationary phase composed of clayey and calcareous sand. It was shown that the transport of strontium was mainly governed by the calcocarbonic chemical equilibria and by Sr/Ca cationic exchange, when the ratio of strontium and calcium concentrations was lower than the ratio of solubility products of strontianite and calcite:

$$[\text{Sr}^{2+}] < [\text{Ca}^{2+}] \frac{P_{\text{SrCO}_3}}{P_{\text{CaCO}_3}} = 0.246[\text{Ca}^{2+}]$$

so avoiding strontianite precipitation and in absence of other cations. The main characteristic of Sr/Ca cation exchange is that the selectivity is close to 1, more exactly 1.05. This indicates that chemical reactivity of calcium and strontium are similar on clay surfaces;  $\text{Ca}^{2+}$  and  $\text{Sr}^{2+}$  are chemical analogues.

The aim of this paper is to check the previous approach under new conditions by experiments where strontium is at trace level in the presence of sodium as a third competitive cation at different concentrations. This approach is so checked under column packing and hydrodynamic conditions exhibiting mass transfer limiting kinetics. In the first part, the theory of ion exchange is used to evaluate the  $K_d$  of  $^{45}\text{Ca}$  and  $^{90}\text{Sr}$  as a function of concentrations of major cations. This calculation allows us to predict variations in  $K_d$  as of function of the chemical conditions, in particular with the ionic composition of the leaching solution. Experiments are performed of the transient transport of  $^{45}\text{Ca}^{2+}$  in conditions where  $\text{Ca}^{2+}/\text{Na}^+$  exchange is expected to occur and the results are compared with predictions from numerical simulations. We also use

$^{45}\text{Ca}^{2+}$  to measure the hydrodynamic properties of the porous medium, especially where there is kinetic mass transfer limitation. In these conditions, we finally check the prediction of Sr transport at trace concentration.

## 2. Working equations

### 2.1. $K_d$ calculation: the cation exchange model

When the physicochemical conditions (composition of leaching solution, temperature and pressure) are maintained constant in a calcareous and clayey sandy soil, the calculation of distribution coefficient,  $K_d$ , of a cation  $M^{z+}$  becomes possible if its concentration  $[M^{z+}]$ , is low with respect to the major cations. In this kind of soil, the exchange capacity of clays is usually saturated with calcium. The sorption of a cation  $M^{z+}$  can be viewed as a competitive adsorption on Ca-clays. The heterogeneous reaction describing this competition is given by the stoichiometric mass balance:

$$\text{Ca}_f + \frac{2}{z} M^{z+} = \text{Ca}^{2+} + \frac{2}{z} M_f \tag{1}$$

where the selectivity coefficient is defined in terms of mass action law by

$$K_{M/\text{Ca}} = \frac{[\text{Ca}^{2+}][M_f]^{2/z}}{[\text{Ca}_f][M^{z+}]^{2/z}} \tag{2a}$$

We use concentrations in mole per litre of pore volume even for the fixed species,  $M_f$ . Typically when a column is saturated with M,  $[M_f]$  is the number of moles of M sorbed on the porous medium divided by the pore volume  $V_p$ . The exchange capacity, Ne, is so given in equivalent per litre of pore volume.

The correspondence with the classical Gaines–Thomas coefficient (Gaines and Thomas, 1953), where the surface composition is defined in term of ionic fraction,  $\bar{x}_M = (z[M_f])/Ne$ , is:

$$K_{M/\text{Ca}} = \frac{2}{z^{2/z}} Ne^{2/z-1} \left( \frac{\bar{x}_M^{2/z} [\text{Ca}]}{\bar{x}_{\text{Ca}} [M]^{2/z}} \right) = \frac{2}{z^{2/z}} Ne^{2/z-1} K_{\text{GTM}/\text{Ca}} \tag{2b}$$

The distribution coefficient of a cation  $M^{z+}$  is by definition:

$$K_{dM} = \frac{[M_f]}{[M^{z+}]} \tag{3a}$$

Note that  $K_{dM}$  is dimensionless in the chosen units. To obtain the classical  $K'_{dM}$  in  $\text{kg}^{-1}$ , the reference volume,  $V_p$ , must be replaced by the concentration of fixed  $M^{z+}$  per mass of soil,  $m$ :

$$K'_{dM} = K_{dM} \frac{V_p}{m} \tag{3b}$$

By substituting  $K_{dM}$  for Eq. 3 into Eq. 2:

$$K_{dM} = \left[ K_{M/Ca} \frac{[Ca_f]}{[Ca^{2+}]} \right]^{z/2} \quad (4a)$$

When the sites of the porous medium are saturated with calcium, the exchange capacity, Ne, in eq per volume of  $V_p$ , is equal to  $2[Ca_f]$ , and:

$$K_{dM} \approx \left[ K_{M/Ca} \frac{Ne}{2[Ca^{2+}]} \right]^{z/2} \quad (4b)$$

The value of  $[Ca^{2+}]$  depends on experimental conditions. If the concentration of calcium is imposed by an artificial injection of calcium chloride at concentrations above  $10^{-3}$  mol  $L^{-1}$ ,  $[Ca^{2+}]$  is close to the imposed concentration. If the concentration of calcium is low or fixed naturally by calcocarbonic equilibria, its calculation must use these equilibria. For instance, in absence of atmospheric  $CO_2$  and in contact with pure water at room temperature the calcium concentration of a solution in contact with a calcareous and clayey sand is  $1.25 \cdot 10^{-4}$  mol  $L^{-1}$  and the pH close to 10 (Schweich and Sardin, 1985).

When the cation being transported is an isotope of calcium,  $Ca^*$ , the charge of cations in competition is identical and the selectivity coefficient is equal to 1. Thus, relationship (4b) becomes:

$$K_d^* = \frac{Ne}{2[Ca^{2+}]} \quad (4c)$$

For strontium, relationship (4b) is written as:

$$K_{dSr} \approx K_{Sr/Ca} \frac{Ne}{2[Ca^{2+}]} \quad (4d)$$

In a system containing sodium as major cation, the selectivity constant can be written with respect to Na. Introducing the calcium distribution coefficient,  $K_{dCa} = ([Ca_f])/[Ca]$ , in the selectivity coefficient formula  $K_{Ca/Na} = ([Ca_f][Na^+]^2)/([Na_f]^2[Ca^{2+}])$ , opposite of  $K_{Na/Ca}$ , we obtain the relationship:

$$[Na^+]^2 K_{dCa} = K_{Ca/Na} (Ne - 2K_{dCa}[Ca^{2+}])^2 \quad (5)$$

The interest of this relationship is that if ion exchange theory, i.e. the mass action law (1), is valid, then measuring  $[Na^+]$ ,  $[Ca^{2+}]$  and  $K_{dCa}$  for each experiment, and plotting  $X = 2K_{dCa}[Ca^{2+}]$  against  $Y = [Na^+]/\sqrt{K_{dCa}}$  will give a straight line with slope  $\sqrt{K_{Ca/Na}}$ . It is so possible to verify the value of the exchange capacity from the abscissa at  $Y = 0$ .

### 3. Transport model

When the flow in the porous medium is close to a piston flow and  $K_{dM}$  is constant in a given experiment, the mean location of the breakthrough curve of  $M^{z+}$  can be

calculated by means of the classical chromatographic approach in terms of retardation time,  $t_R$ :

$$t_R = \frac{V_p}{Q} (1 + K') \quad (6a)$$

Here, the capacity factor,  $K'$ , is equal to  $K_{dM}$  as a consequence of the choice of reference volume for the concentrations on the solid [relationship (3b)].

At constant flow rate we use the reduced retardation volume,  $v_R$ , that is the ratio of the mean retardation volume of  $M^{z+}$ ,  $V_R$ , to  $V_p$ , the pore volume. For an instantaneous pulse injection, the mean location of the restored peak is given by:

$$v_R = \frac{V_R}{V_p} = \frac{Qt_R}{Qt_0} = 1 + K_{dM} \quad (6b)$$

If the pulse duration of injection is not negligible the mean location of peak becomes:

$$v_R = \frac{1}{2}v_1 + 1 + K_{dM} \quad (6c)$$

where  $v_1$  is the reduced injected volume (4th column of Table 3).

Relationships (6a) and (6b) allow us to predict the location of the breakthrough curve of the species  $M^{z+}$  when  $K_{dM}$  is constant.

The model of mixing cells in series (Villiermaux, 1982) has been chosen to take into account the dispersivity of the flow. In this model, the number of mixing cells,  $J$ , is related to the axial dispersion coefficient,  $D_A$ , by the simple expression:

$$J = \frac{Pe}{2} = \frac{uL}{2D_A} = \frac{L}{\alpha} \quad (7a)$$

where  $Pe$  is the Péclet number;  $u$  the interstitial flow velocity (pore velocity);  $L$  the length of the porous medium; and  $\alpha$  the dispersivity. In the case of a pure dispersive–convective flow the number  $J$  can be calculated from the variance,  $\sigma^2$ , of the response to an instantaneous pulse injection by:

$$J = \frac{t_R^2}{\sigma^2} \quad (7b)$$

Sardin et al. (1991) showed how to model these phenomena for linearly interacting solutes in the presence of mass transfer kinetics. Generally, using a first-order approximation to represent the kinetics is sufficient to give a good image of the observed behaviour. Limitations by mass transfer kinetics do not modify relationship (6a) which remains valid; the mean retention time of a given solute depends only on thermodynamics. The consequences of kinetic limitations can be seen by the study of the variance of breakthrough curves from tracer tests at different flow rates. With respect to the classical convective–dispersive model, the reduced variance is given by  $\sigma'^2 = 1/J$  and is

independent of flow rate when the hydrodynamic dispersion phenomenon prevails. The assumption of a first-order kinetic limitation process introduces a new term in the expression of the reduced variance, involving a new parameter, the characteristic transfer time,  $t_M$ :

$$\sigma'^2 = \frac{1}{J} + \frac{2K'}{1+K'} \frac{t_M}{t_R} = \frac{1}{J} + \frac{2K'}{(1+K')^2} \frac{t_M}{V_p} Q \quad (8)$$

Plotting  $\sigma'^2$  against the flow rate gives a straight line. Relationship (6b) gives the value of  $K'$  which is equal to  $K_{dM}$ . The slope of the straight line and the value of  $\sigma'^2$  when  $Q = 0$ , give access to the values of  $t_M$  and  $J$ .

Finally, to check the validity of the approach in terms of  $K_d$ , the IMPACT code (Jauzein et al., 1989) is used to numerically solve the system of equations describing hydrodynamic, speciation (calcocarbonic equilibria), and ionic exchange, and to calculate the breakthrough curve of the radionuclide. The hydrodynamic parameters introduced in the model,  $V_p$  and  $J$ , are measured independently from the breakthrough curve of a step injection of calcium chloride (Sardin et al., 1986).

## 4. Experimental

### 4.1. Operating conditions, soil characteristics

The experiments have been performed on three columns that were filled with the same relative proportions of the components (Table 1). Two procedures have been used to prepare the mixture of minerals. The first procedure gives an artificial soil,  $S_1$  soil, and consists in wet mixing silica, calcite and clay in 0.05 M  $\text{CaCl}_2$  solution. Then the mixture is dried at a low temperature (40°C). The second procedure leads to the  $S_2$  soil where the same three mineral components are mechanically mixed when dry. Two columns, A and B, are filled with the  $S_1$  soil and one column, C, with the  $S_2$  soil. Before being used, the columns are purged of air with  $\text{CO}_2$  as purging gas and saturated with 0.05 M  $\text{CaCl}_2$  solution to put the exchange sites of the clays in calcium form. The responses to step variations of  $\text{CaCl}_2$ , which is well suited to trace the flow in the given

Table 1  
Mineral composition of sand

Soil composition	% weight	Clays (< 2 $\mu\text{m}$ composition)	% weight
Silica	97.26	Quartz	7
Calcite	1.78	Goethite	6
Clays (FOCA7)	0.96	Calcite	2
		Kaolinite	5
		(50% kaolinite, 50% smectite)	80

Table 2  
Soil column characteristics

	Column			
	A	B	C	
Inner diameter (cm)	1.6	0.9	0.9	
Length of bed (cm)	7.5	13	16.1	
Type of sand	S <sub>1</sub>	S <sub>1</sub>	S <sub>2</sub>	
Mass of sand (g)	19.5	12	15	
Pore volume (cm <sup>3</sup> )	7.6	4.3	5.2	
Porosity	0.50	0.52	0.51	
Number of mixing cells, <i>J</i> (water tracer)	131	70	40	
Dispersivity, $\alpha = L/2J$ (cm)	0.029	0.093	0.20	
Flow rate (cm <sup>3</sup> min <sup>-1</sup> )	1.0	1.0	0.003	1.0
Mass transfer kinetics				
$J = 40, t_M =$			18.9	2.13
$J = 18, t_M =$			1.56	1.56
Exchange capacity ( $\mu\text{eq g}^{-1}$ )	13.3	13.4	7.6	

experimental conditions (Sardin et al., 1986), are measured by conductivity at the outlet of the column. The first and the second moments of these responses give access to the pore volume  $V_p$  and the dispersion of the flow (number of mixing cells,  $J$ , and the dispersivity,  $\alpha$ ). Table 2 gives the characteristics of the three columns as well as the parameters of the flow model,  $V_p$  and  $J$ . It should be noted that the best packing is obtained with the column A ( $\alpha = 0.029$  cm) and the worst with column C.

#### 4.2. Measurement of the exchange capacity

The exchange capacity of the soil is measured by interpreting the elution curve of a injection pulse of <sup>45</sup>Ca tracer in a column feed with calcium chloride only. The injected tracer solution is of the same chemical composition as the pre-equilibrating solution and the eluent. This means that Eq. 4c can be used. This method has also been used successfully by Schaefer (1991) to determine the exchange capacity of quartz. We verify that the exchange capacities of columns A and B, which are filled with the S<sub>1</sub> soil, are the same; they differ by less than 1% (Table 2). On the other hand, there is a significant difference between the results of exchange capacity measurements of the porous media S<sub>1</sub> and S<sub>2</sub> (13.4 and 7.6  $\mu\text{eq g}^{-1}$ , respectively). This can be explained by the distribution of clays inside the mixture. In S<sub>1</sub> this is homogeneous, and the sand appears light-brown coloured clay, whereas S<sub>2</sub> has the white colour of the quartz and some aggregates of clays can be easily seen. Observation with an optical microscope confirms that S<sub>1</sub> is composed of 100–250- $\mu\text{m}$  particles, whereas S<sub>2</sub> also contains clay aggregates and small ( $\sim 1$  mm) particles mainly of clay. This suggests that when the mixture is prepared by the wet method, clay particles spread around the sand grains and the exchange sites are more accessible.

## 5. Results, interpretation and discussion

### 5.1. $\text{Ca}^{2+} / \text{Na}^+$ exchange

For the set of experiments Nos. 1–10 (Table 3), the pre-equilibration, injection and elution solutions have the same NaCl and  $\text{CaCl}_2$  concentrations which are maintained constant during a single experiment.  $^{45}\text{Ca}$  is added to the injection solution and measured at the outlet of the column. We have chosen this procedure and these chemical conditions to be able to apply Eq. 5.

In the absence of sodium chloride (exp. 1, Fig. 1), the  $^{45}\text{Ca}$  elution peak leaves the column after  $16.4V_p$  (Table 3) and not after  $1V_p$  as would a tracer for water. This is due to Ca self-exchange ( $^{45}\text{Ca}/\text{Ca}$ ), and depends only on the exchange capacity of the stationary phase. Using Eq. 5 with  $[\text{Na}] = 0$  gives exchange capacity by  $\text{Ne} = 2K_{\text{dCa}}[\text{Ca}^{2+}]$  (see Eq. 4c).

When the concentration of sodium chloride increases, the  $^{45}\text{Ca}$  elution peak is shifted toward smaller elution volumes (exps. 2 and 3, Fig. 1). This is obviously due to the competition between the two cations for the exchange sites of the porous medium: only a part of the exchange capacity can now be reached by Ca. An excess of NaCl has to be used to see this effect, because the chemical reactivity of  $\text{Na}^+$  for the porous medium is smaller than that of  $\text{Ca}^{2+}$ .

A value of the constant of ionic exchange equilibrium is then calculated by using Eq. 5 for each experiment. All these values are the same within the experimental uncertainty. This is shown by plotting the straight line of Eq. 5 with the experimental results (Fig. 2). The slope gives  $K_{\text{Ca}/\text{Na}} = 104$  and  $K_{\text{GTCa}/\text{Na}} = 6.9$ , values which are in

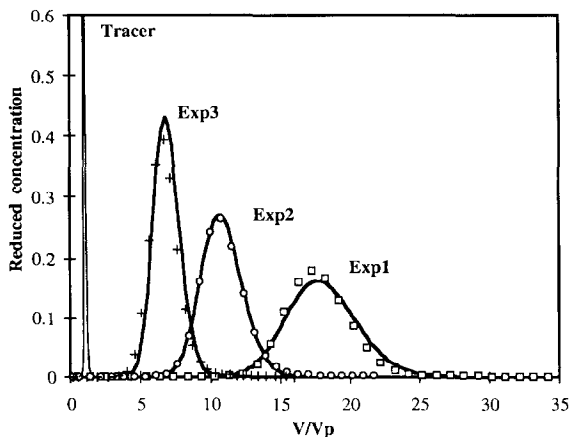


Fig. 1. Influence of NaCl concentration on  $^{45}\text{Ca}$  breakthrough curves. Experiments 1–3 are performed in column A (see Table 3). Total NaCl and  $\text{CaCl}_2$  concentrations are constant during a given experiment.  $K_{\text{dCa}}$  is deduced from the mean position of the elution peak (Eq. 6c). Simulations with IMPACT code (Jauzein et al., 1989):  $J = 131$ ,  $V_p = 7.6$ ,  $\text{Ne} = 0.034 \text{ eq L}^{-1}$ ,  $K_{\text{Ca}/\text{Na}} = 104$  ( $K_{\text{GTCa}/\text{Na}} = 6.9$ ), calcocarbonic equilibria (Lefèvre et al., 1993), reference compositions: Table 3.

Table 3

Experimental conditions: reduced injected volumes, composition of leached solutions and reduced restitution volumes

Run	Column	Major cations composition in pre-equilibration, pulse and driving solution (M)	$\nu_1$	Tracer in pulse or composition if different	$\nu_R$
1	A	$\text{CaCl}_2 10^{-3}$	1.06	$^{45}\text{Ca}$	17.82
2	A	$\text{CaCl}_2 10^{-3}, \text{NaCl } 5 \cdot 10^{-2}$	1.00	$^{45}\text{Ca}$	11.0
3	A	$\text{CaCl}_2 10^{-3}, \text{NaCl } 10^{-1}$	0.78	$^{45}\text{Ca}$	6.37
4	B	$\text{CaCl}_2 10^{-3}$	1.05	$^{45}\text{Ca}$	19.45
5	B	$\text{CaCl}_2 10^{-3}, \text{NaCl } 10^{-2}$	1.10	$^{45}\text{Ca}$	17.68
6	B	$\text{CaCl}_2 10^{-3}, \text{NaCl } 2 \cdot 10^{-2}$	1.01	$^{45}\text{Ca}$	15.73
7	B	$\text{CaCl}_2 2 \cdot 10^{-3}, \text{NaCl } 10^{-2}$	1.03	$^{45}\text{Ca}$	9.84
8	B	$\text{CaCl}_2 4 \cdot 10^{-3}, \text{NaCl } 10^{-2}$	1.07	$^{45}\text{Ca}$	5.90
9	B	$\text{CaCl}_2 5 \cdot 10^{-4}, \text{NaCl } 10^{-1}$	1.02	$^{45}\text{Ca}$	8.51
10	B	$\text{CaCl}_2 2 \cdot 10^{-3}, \text{NaCl } 10^{-1}$	1.05	$^{45}\text{Ca}$	5.58
11	C	$\text{CaCl}_2 2 \cdot 10^{-3}$	2.01	$^{45}\text{Ca}$	7.32
12	C	$\text{CaCl}_2 2 \cdot 10^{-3}$	1.86	$^{45}\text{Ca}$	7.07
13	C	$\text{CaCl}_2 5 \cdot 10^{-3}$	2.00	$^{45}\text{Ca}$	4.19
14	C	$\text{CaCl}_2 5 \cdot 10^{-3}$	1.98	$\text{CaCl}_2 4.9 \cdot 10^{-3}, \text{SrCl}_2 10^{-4}, ^{90}\text{Sr}$	4.25
15	C	$\text{CaCl}_2 5 \cdot 10^{-3}$	1.91	$^{90}\text{Sr } 2.6 \cdot 10^{-8}$	4.23
16	C	$\text{CaCl}_2 5 \cdot 10^{-3}$	1.84	$^{90}\text{Sr } 2.6 \cdot 10^{-9}$	4.23

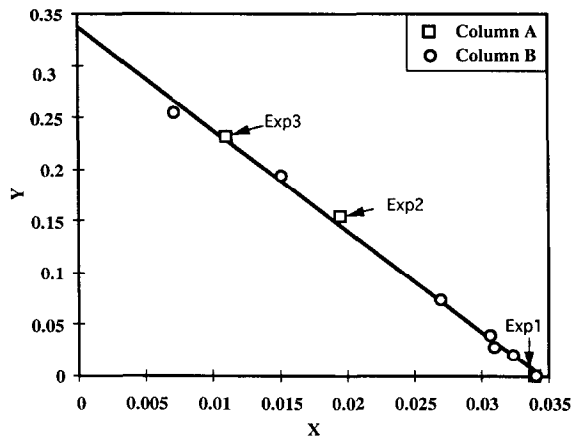


Fig. 2. Determination of the Ca/Na cationic exchange constant. The exchange capacity,  $N_e = 0.034 \text{ eq L}^{-1}$ , is calculated from  $^{45}\text{Ca}/\text{Ca}$  exchange experiment. The characteristics of the column are given in Table 2 and the experimental conditions are given in Table 3:  $\square$  = column A, experiments 1–3;  $\circ$  = column B: experiments 4–10.  $K_{\text{dCa}} = \nu_R - \frac{1}{2}\nu_1 - 1$ ;  $X = 2K_{\text{dCa}} [\text{Ca}^{2+}] \text{ (eq L}^{-1}\text{)}$  and  $Y = \sqrt{K_{\text{dCa}}} [\text{Na}^+] \text{ (eq L}^{-1}\text{)}$ .  $K_{\text{Ca}/\text{Na}} = 104$  is calculated from the slope of the straight line (see Eq. 5).

Table 4

Gaines–Thomas selectivity coefficient from the literature for exchange  $\text{Ca}^{2+} / \text{Na}^{+}$  on clayey minerals

Soil	Exchange capacity ( $\mu\text{eq g}^{-1}$ )	Experimental method	$K_{\text{GTCa/Na}}$ ( $\text{mol L}^{-1}$ )	Reference
Montmorillonite	354	batch	48	Gheyi and van Bladel (1975)
Illite/kaolinite	277	batch	12	Gheyi and van Bladel (1975)
Kaolinite	255	batch	21	Gheyi and van Bladel (1975)
Various soils		batch	6–13	Bolt (1982)
Sand of Güe	8.4	column	6.3	Sardin et al. (1986)
Sand of Chateurenard	7.4	column	13	Schweich and Sardin (1985)
Sediment	100	column	6	Valocchi et al. (1981)
Sediment	18	column	8	Jauzein et al. (1989)
Artificial mixture	13.4	column	6.9	present work

reasonable agreement with those from the literature (Table 4). When we use the constant value deduced from Fig. 2 to model the experiments presented in Fig. 1 with the IMPACT code, the predicted position and the shape of the breakthrough curves are in good agreement with these results.

The possibility of simulating experiments performed over a large domain of ionic compositions, with the same set of coefficients confirms the predominant role of cationic exchange in the retention of radiocalcium. In this type of experiment, where  $K_d$  is constant, the exchange constant can then be used to predict the mean retention volumes of experiments. Note that in other chemical conditions, other equilibria could interfere with the above mechanism, for example, calcium complexation in aqueous solution and competition with  $\text{H}^+$  ions.

### 5.2. Kinetic limitations

The kinetic limitations are investigated with the column C ( $\text{S}_2$  soil) by performing experiments at two different flow rates (2 and  $60 \text{ cm}^3 \text{ h}^{-1}$ ). Chemical complications have been avoided by using Ca self-exchange. As the flow rate increases the breakthrough curves (Fig. 3) broaden and the peak height decreases. Note that each curve also becomes slightly less symmetrical (there is more tailing) and that its peak maximum is slightly shifted toward shorter elution volumes. This type of behaviour is generally observed when first-order mass transfer kinetics is the limiting process. The local equilibrium assumption is no longer valid.

Theoretical breakthrough curves have been simulated with a first-order kinetic law assuming constant  $K_d$  and a mass transfer limitation of the solute (here  $^{45}\text{Ca}$ ) to, or into, the porous medium. The reduced characteristic mass transfer time,  $t_M$ , is deduced by curves fitting after each experiment. Two assumptions can be introduced to evaluate  $t_M$ . First, we assume that the dispersion of the interactive tracer is the same as that for the water tracer. In expression (8),  $J$  and  $K'$  are given and only  $t_M$  is fitted. In this case, we

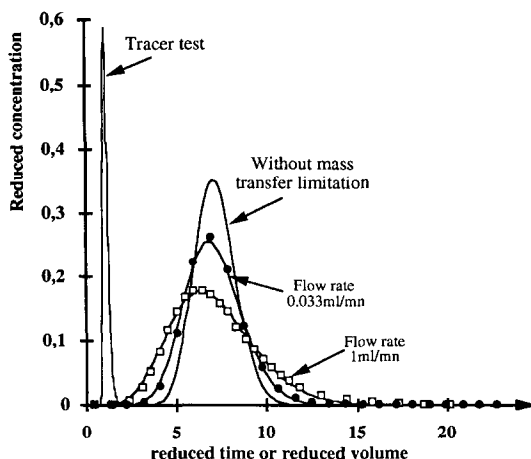


Fig. 3. Influence of the flow rate on the breakthrough curve shape of radiocalcium. Injection of a rectangular step of radiocalcium at  $2 \cdot 10^{-3} M$  (exps. 11 and 12, Table 3). The points represent experiments in column C at two different flow rates: ●,  $Q = 0.033 \text{ cm}^3 \text{ min}^{-1}$ ; □,  $Q = 1.0 \text{ cm}^3 \text{ min}^{-1}$ . Simulations with a linear model:  $J = 40$ ,  $K' = 5.1$ .

obtain two different value of  $t_M$ , indicating that the model is not well suited to the observed behaviour, even if the calculated curves with these values are in good agreement with the experimental data (Fig. 3). The second assumption consists in fitting the model with two parameters,  $J$  and  $t_M$ . From the two curves at different flow rates one set of parameters is found:  $J = 18$  and  $t_M = 1.56 \text{ min}$ . The curves simulated from this set of parameters cannot be distinguished from the previous ones. The fact that two sets of parameters simulate the same curve is well known and has been described by Villermaux and Antoine (1978). It is due to the difficult in distinguishing between dispersion and mass transfer kinetics when the mass transfer characteristic,  $t_M$ , remains low with respect to the convective time,  $V_p/Q$ . This second assumption means that the dispersion of the interactive tracer is different from that of the water tracer. More experiments over a large range of flow rates would be needed to discriminate between these two assumptions.

### 5.3. Transport of strontium

We have previously (Lefèvre et al., 1993) studied strontium in the same type of chromatographic set up and we have measured the ionic exchange equilibrium constant,  $K_{\text{Ca/Sr}} = 1.05$ . This value is to be compared with those obtained by Heald (1960) in batch experiments on four clays. The values of  $K_{\text{Ca/Sr}}$  lie between 0.99 and 1.34. Heald did not find a good agreement at low concentrations and he interpreted this by supposing that there were two independent adsorption sites. However, he did not characterise the second site which represented  $< 1\%$  of the exchange capacity.

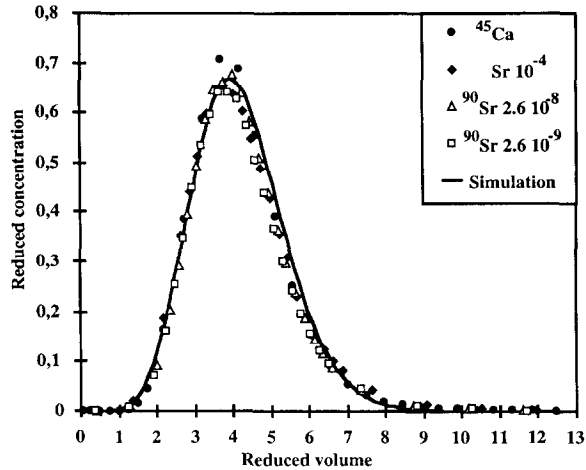


Fig. 4. Experimental verification of prediction of Sr transport for Sr concentrations going from  $2.6 \cdot 10^{-9}$  to  $10^{-4}$  M. Sr is injected and eluted with  $5 \cdot 10^{-3}$  M  $\text{CaCl}_2$  solution. Experiments 13–16 are performed in column C. The simulation is performed with the linear model taking into account mass transfer kinetics:  $J = 40$ ;  $t_M = 2.13$  min,  $K' = 1.8$ ,  $Q = 1$  cm<sup>3</sup> min<sup>-1</sup>.

We have used a radioactive tracer to check our previous results for lower Sr concentration. We have also extended our study to hydrodynamic conditions similar to those described in the previous paragraph. The results presented in Fig. 4 show that the location of the strontium peak is independent of the injected concentration whatever the injection concentration. This behaviour is characteristic of a linear process. In conditions where the calcium chloride concentration is carefully maintained at  $5 \cdot 10^{-3}$ , the partition coefficient remains constant. The prediction of the kinetic model fits perfectly with the experimental results and there is no effect due to lowering the Sr concentration.

## 6. Conclusions

Maintaining constant chemical conditions during a single chromatographic experiment, is a convenient method for determining the value of the distribution coefficient of a radioelement in a given soil. The mineral analysis of the soil (presence of calcite and clays) determines the choice of the predominant heterogeneous reactions, which must be accounted for to give good predictions of the  $K_d$  variations with the chemical conditions. In a calcareous and clayey sandy soil, for Na, Ca and Sr, these are ion exchange and calcocarbonic equilibria. Knowing the composition of the leaching solution and the values of ion exchange coefficients allows an a priori calculation of the distribution coefficient. This approach could certainly be extended to more complicated coupled equilibria in aqueous solution and on the surface of the porous medium, for instance, surface complexation or multisite systems.

We have shown that the previous approach can also be used when piston flow conditions are not obtained: convective–dispersive flow with local equilibrium assumption and convective–dispersive flow with mass transfer kinetics. The hydrodynamic characteristics of the porous medium can be measured independently with a water tracer.

## 7. Notation

$K_{M/Ca}$	selectivity coefficient (dimensionless) of the cationic exchange, see Eq. 2a
$K_{GTM/Ca}$	Gaines–Thomas selectivity coefficient, see Eq. 2b
$K'$	capacity factor (dimensionless) = $K_d$
$K_{dM}$	distribution coefficient (dimensionless) of M between mobile and stationary phases, see Eqs. 3 and 6
$K_d^*$	distribution coefficient of $^{45}\text{Ca}$
$m$	mass of sand (kg)
$[M_f], [\bar{M}]$	concentration (mol L $^{-1}$ ) of $M^{z+}$ species fixed on the porous medium, see Eq. 2a
$[M^{z+}]$	concentration (mol L $^{-1}$ ) of species $M^{z+}$
Ne	cationic exchange capacity (eq/litre of pore volume), see Eq. 2b
$J$	number of mixing cells
Pe	Péclet number [ $= (uL)/(D_A)$ ] (dimensionless)
$Q$	flow rate (mL min $^{-1}$ )
$t_0, t_R$	convection time and retention time, respectively (min)
$t_M$	mass transfer time (min), see Eq. 8
$u$	pore velocity (cm min $^{-1}$ )
$V_1, v_1$	injected volume (L) and reduced injected volume ( $V_1/V_p$ ), respectively
$V_p$	pore volume (cm $^3$ )
$V_R$	retardation volume (cm $^3$ )
$v_R$	reduced retardation volume, $V_R/V_p$
$\bar{x}_M$	ionic fraction of $M^{z+}$ on the solid (dimensionless)

### *Greek symbols:*

$\alpha$	dispersivity (cm)
$\sigma^2, \sigma'^2$	variance (min) (Eq. 7b) and reduced variance (dimensionless) (Eq. 8), respectively

## References

- Bolt, G.H. (Editor), 1982. Soil Chemistry, B. Physico-chemical Models. Elsevier, Amsterdam, 527 pp.
- Gaines, L.G. and Thomas, H.C., 1953. Adsorption studies on clay minerals, II-A. Formulation of the thermodynamics of ion exchange adsorption. J. Chem. Eng., 21: 714–718.

- Gheyi, H.R. and van Bladel, R., 1975. Calcium–sodium and calcium–magnesium exchange equilibria on some calcareous soils and a montmorillonite clay. *Agrochimica*, 19(6).
- Heald, W.R., 1960. Characterization of exchange reactions of strontium or calcium on four clays. *Soil Sci. Soc. Am., Proc.*, 24: 103–106.
- Jaouzein, M., André, C., Margrita, R. and Sardin, M., 1989. A flexible computer code for modelling transport in porous media: Impact. *Geoderma*, 44: 95–113.
- Lefèvre, F., Sardin, M. and Schweich, D., 1993. Migration of strontium in clayey and calcareous sandy oil: precipitation and ion exchange. In: J.I. Kim and G. de Marsily (Editors), *Chemistry and Migration of Actinides and Fission Products*. *J. Contam. Hydrol.*, 13: 215–229 (special issue).
- Sardin, M., Krebs, R. and Schweich, D., 1986. Transient mass transport in the presence of non-linear physico-chemical interaction laws: progressive modelling and appropriate experimental procedures. *Geoderma*, 38: 115–130.
- Sardin, M., Schweich, D., Leij, F. and van Genuchten, M.Th., 1991. Modeling the nonequilibrium transport of linearly interacting solutes in porous media: a review. *Water Resour. Res.* 27(29): 2287–2307.
- Schaefer, K.W., 1991. Determination of the  $\text{Ca}^{2+}$  sorption capacity of quartz surface using  $^{45}\text{Ca}$  as tracer: a column experiment. *Radiochim. Acta*, 54: 47–51.
- Schweich, D. and Sardin, M., 1981. Adsorption, partition, ion exchange and chemical reaction in batch reactors or in columns: a review. *J. Hydrol.*, 50: 1–33.
- Schweich, D. and Sardin, M., 1985. Transient ion exchange and solubilization of limestone in an oil field sandstone: experimental and theoretical wavefront analysis. *AIChE (Am. Inst. Chem. Eng.) J.*, 31(11): 1882–1890.
- Valocchi, A.J., Street, R.L. and Roberts, P.V., 1981. Transport of ion-exchanging solutes in groundwater: chromatographic theory and field simulation. *Water Resour. Res.*, 17(5): 1517–1527.
- Villiermaux, J., 1982. *Génie de la réaction chimique; conception et fonctionnement des réacteurs*. Lavoisier Tec&Doc, Paris, 401 pp.
- Villiermaux, J. and Antoine, B., 1978. Construction et ajustement des modèles mathématiques: une science ou un art? *Bull. BRGM (Bur. Rech. Géol. Min.)*, 2(III, 4): 327–339.